

FIG. 4. Experimental Nusselt number vs Rayleigh number for various positions of the partition.

The results of the experiments are shown in Fig. 3 in which the Nusselt number is expressed as a function of the Rayleigh number. The Nusselt numbers for a given Rayleigh number are independent of various values of W'/W for the values of $H/W = 4$ and 10. Also, all of experimental data agree well with the boundary layer solution presented previously for the case of a central partition. Under these experimental conditions, the width of each cell constructed by the partition is larger than the minimum width calculated using equation (2), and thus the premise described in Section 2 is valid.

4. NUMERICAL COMPUTATION

A theoretical investigation was carried out to confirm the validity of equation (2) using a two-dimensional Galerkin finite element method. The solution technique is the same as that previously used [8]. The equations utilized were the Navier-Stokes and the energy transport equations. The computation was performed in the range $10^3 < Ra < 10^6$ for $Pr = 6$ and $H/W = 4$. Solutions were obtained for different positions of the partition from the center of the enclosure to the cold wall ($W'/W < 0.5$). Because the experimental Nusselt numbers are essentially identical whether the position of the partition is located at the cold or hot wall side as shown in Fig. 3.

Figure 4 shows the calculated results of the Nusselt number as a function of the Rayleigh number. In this case, Nusselt numbers for various values of W'/W deviate from the boundary layer solution, particularly for Rayleigh numbers less than 10^5 . Equation (2) predicts that the boundary layer approximation is satisfied for W'/W larger than 0.418 at $Ra = 10^5$. This agrees with the results of the numerical computation at $Ra = 10^5$.

Thus the validity of equation (2) is considered to be confirmed both by experimental measurement and numerical computation as indicated above.

Acknowledgements—The authors acknowledge with thanks the assistance of Mr Masayuki Yamamoto with the experi-

ments. This work was supported in part by a Grant-in-Aid for Scientific Research (No. 61750891) from the Ministry of Education, Science and Culture of Japan. We are also very grateful for the revision in the English text by Professor W. Hayduk of the University of Ottawa.

REFERENCES

1. I. Catton, Natural convection in enclosures, *Proc. 6th Int. Heat Transfer Conference*, Vol. 6, pp. 13–43 (1978).
2. S. W. Churchill, Free convection in layers and enclosures. In *Heat Exchanger Design Handbook*, Chap. 2.5.8. Hemisphere, Washington, DC (1983).
3. D. Duxbury, An interferometric study of natural convection in enclosed plane air layers with complete and partial central vertical divisions, Ph.D. Thesis, University of Salford (1979).
4. H. Nakamura, Y. Asako and T. Hirata, Natural convection and thermal radiation in enclosures with partition plate, *Trans. JSME Ser. B*, **50**, 2647–2654 (1984).
5. T. Nishimura, M. Shiraishi and Y. Kawamura, Analysis of natural convection heat transfer in enclosures divided by a vertical partition plate, *Proc. Int. Symp. Heat Transfer*, Beijing, Paper No. 85-ISHT-1-6 (1985).
6. T. W. Tong and F. M. Gerner, Natural convection in partitioned air-filled rectangular enclosures, *Int. Commun. Heat Mass Transfer* **13**, 99–108 (1986).
7. T. Nishimura, T. Takumi, Y. Kawamura and H. Ozoe, Experiments of natural convection heat transfer in rectangular enclosure partially filled with particles, *Kagaku Kogaku Ronbunshu* **11**, 405–411 (1985); *Heat Transfer—Jap. Res.* **15**, 62–76 (1986).
8. T. Nishimura, T. Takumi, M. Shiraishi, Y. Kawamura and H. Ozoe, Numerical analysis of natural convection in a rectangular enclosure horizontally divided into fluid and porous regions, *Int. J. Heat Mass Transfer* **29**, 889–898 (1986).

A generalized correlation for thermal design data of heat-pipe heat exchangers

SHOU-SHING HSIEH

Department of Mechanical Engineering, National Sun Yat-Sen University,
Kaohsiung, Taiwan 80424, Republic of China

(Received 16 May 1986 and in final form 30 January 1987)

INTRODUCTION

HEAT EXCHANGERS made of heat pipes have attracted much attention in the application of economic devices for the

recovery of waste heat energy [1–3]. Although the characteristics of thermal performance of a single heat pipe have been extensively studied and clearly understood during the past 20 years, the study of the overall performance of heat

NOMENCLATURE

<p>A heat transfer area of heat exchanger ($W \times H$) [m] C constant, $(AU\Delta T_m)^{-1}$ [W^{-1}] c_1, c_2 correlation constants related to heat transfer rate of heat-pipe heat exchanger g_1 correlation constant related to mass flux of heat-pipe heat exchanger [$kg\ s^{-1}$] g_2 correlation constant related to mass flux of heat-pipe heat exchanger [$kg\ s^{-1}$] H height of the side cross-sectional area considered as a unit cell [m] \dot{m}_t total mass flux of the present configuration considered as a single heat pipe [$kg\ s^{-1}$] \dot{m}_v total mass flux of heat-pipe heat exchanger [$kg\ s^{-1}$] $\dot{m}_{v,j}$ mass flux passing through the jth column of heat pipes [$kg\ s^{-1}$] Q heat transfer rate of heat-pipe heat exchanger [W] Q_s heat transfer rate of the present system considered as a single heat pipe [W]</p>	<p>Q_0 heat transfer rate of present system without heat pipe [W] $q_{p,j}$ heat transfer rate in the jth column of heat pipes [W] T temperature [$^{\circ}C$] ΔT_m log mean temperature difference when the present configuration was used as an ordinary heat exchanger [$^{\circ}C$] U overall heat transfer coefficient [$W\ m^{-2}\ ^{\circ}C^{-1}$], $20\ W\ m^{-2}\ ^{\circ}C^{-1}$ presently used W width of the side cross-sectional area considered as a unit cell [m].</p> <p>Subscripts c condenser side; cold air h evaporator side; hot air j jth column of heat pipe m logarithmic mean.</p>
---	---

exchangers with a heat-pipe bank as the heat transfer elements appears to be limited. Most recently, Huang and Tsuei [4] presented an analytical method for the prediction of the thermal performance of such heat exchangers based on the conductance model in which the specific heat conductance of the heat pipe was obtained from a performance test of a single heat pipe. In spite of this, the general picture of the thermal performance of a bank of heat pipes with different alignments applied to waste heat recovery system design seems underdeveloped. In this paper a simplified but relatively generalized method is proposed and the results can be directly used for the design and the performance test of the bank type heat-pipe heat exchangers applicable to waste heat recovery system configurations.

FUNDAMENTAL BACKGROUND

A conventional counter-flow heat exchanger using heat pipes is shown in Fig. 1. The total heat Q transferred for the heat exchanger can theoretically be expressed as

$$Q = \dot{m}_v \bar{h}_{fg} = \sum_{j=1}^{N_c} q_{p,j} \tag{1}$$

where

$$\bar{h}_{fg} = \frac{1}{2} \left(\sum_j^{N_c} h_{fg(h,j)} + \sum_j^{N_c} h_{fg(c,j)} \right) = \sum_{j=1}^{N_c} h_{fg,j}$$

$$\dot{m}_v = \sum_j^{N_c} \dot{m}_{v,j}, \quad \dot{m}_{v,j} = \frac{q_{p,j}}{h_{fg,j}}$$

$$h_{fg,j} = \frac{1}{2} (h_{fg(h)} + h_{fg(c)}).$$

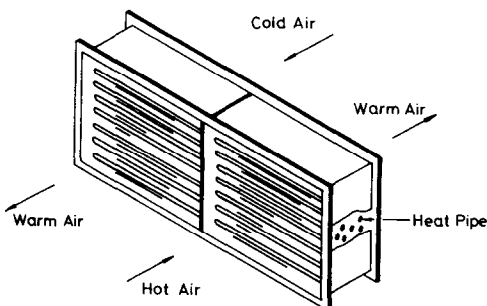


FIG. 1. Typical conventional heat-pipe heat exchanger for a waste heat recovery system.

Whereas the heat transfer caused by a conventional counter-flow heat exchanger without a heat pipe is

$$Q_0 = AU\Delta T_m. \tag{2}$$

Therefore, the ratio of heat transfer due to two different types of heat exchangers can be written as

$$\frac{Q}{Q_0} = \frac{\dot{m}_v h_{fg}}{AU\Delta T_m} = C \bar{h}_{fg} \dot{m}_t \frac{\dot{m}_v}{\dot{m}_t} = c_1 \frac{\dot{m}_v}{\dot{m}_t} \tag{3}$$

where

$$\dot{m}_t = \frac{Q_s}{\frac{1}{2} [h_{fg(h)} + h_{fg(c)}]}$$

$$C = (AU\Delta T_m)^{-1},$$

$$c_1 = C \bar{h}_{fg} \dot{m}_t.$$

It seems that, \dot{m}_v/\dot{m}_t can be expressed in the form of $(1 - e^{-\epsilon_v})$ in which ϵ_v is a fraction of the heat pipe cross-sectional area per unit area basis. This functional relation will be verified in the next section. Equation (3) can therefore be written as

$$\frac{Q}{Q_0} = c_1 (1 - e^{-\epsilon_v}). \tag{4}$$

This indicates that the thermal performance of a heat-pipe heat exchanger can be predicted once c_1 and c_2 are determined for any different staggered heat-pipe alignments.

NUMERICAL CALCULATIONS FOR HEAT TRANSFER RATE AND MASS FLOW RATE

A finite-difference method based on the conductance model is employed in the present study to analyze the overall heat transfer rate of the heat-pipe heat exchanger. Assume that the heat exchanger of rectangular cross-section (2.0×2.2 m in dimension) can be arranged in such a way that the area fraction ϵ_v of the heat exchanger increases from 0.001 to 0.20 for a total of 36 alignments. Two of the typical alignments of the heat exchangers are shown in Fig. 2 and detailed specifications of the heat exchanger used in the present study are depicted in Table 1.

Based on the work of Huang and Tsuei [4], a computer program was developed to calculate the thermal performance and total mass flow rate of the fluid passing through the heat pipes of the heat exchangers of different area fraction ϵ_v s. Before the above-mentioned work was accomplished, the

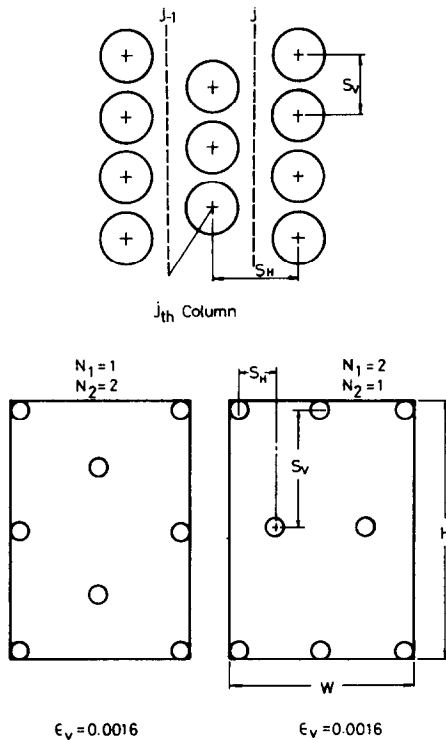


FIG. 2. Schematic diagram of the present heat-pipe heat exchanger and an illustration of different alignments at the same ϵ_v .

computer program was validated by using the same working conditions and physical configuration of the heat-pipe heat exchanger in ref. [4]. Furthermore, the heat transfer rates Q_{0s} of the corresponding conventional counter-type heat exchangers under the same working conditions were also calculated through a typical iterative procedure to provide baseline data.

Through the simple conductance model developed in ref. [3] Q_s was found to calculate the total thermal conductance (UA) of the heat pipe which is found to be $47.98 \text{ W } ^\circ\text{C}^{-1}$. The concept of hydraulic diameter was employed instead of the physical dimension of the present configuration to simulate its diameter when the present waste heat recovery system was considered as a single heat pipe.

Since the specification of the present single heat pipe was similar to that of ref. [4], ten out of twelve test runs in ref.

[4] shown in Table 2 were randomly chosen to calculate the thermal performance of heat-pipe heat exchangers and the total mass flow rate of the fluid passing through these heat pipes.

RESULTS AND DISCUSSION

For the heat transfer performance test, ten out of twelve numerical predictions for different ϵ_v s from ref. [4] have been taken and data were plotted as a function of ϵ_v . The corresponding data was also taken for the condition when they are only considered as a simple heat exchanger without heat pipes. The representative results are shown in Fig. 3. Apparently, the heat transfer rate is different from each other due to the different flow patterns in the present study even though the area fraction of the heat pipe alignment is the same as can be seen in Fig. 3. At the lowest value of ϵ_v , a low heat transfer rate is followed by a monotonical rise to its maximum value, and then approaches a nearly constant value as ϵ_v increases. Therefore, the heat transfer rate seems to be proportional to the number of heat pipes until a certain value of ϵ_v is reached. The reason is that the heat transfer mechanism for low and high ϵ_v s is different. The major heat transfer rate distribution is due to the number of heat pipes used under certain low to moderate ϵ_v s. However, for some larger ϵ_v s, the heat transfer rate is mainly dependent on the flow pattern external to the heat pipe. The thermal performance of baseline data is also indicated in Fig. 3 in which the heat transfer rate for each case is found in between the minimum value at the lowest ϵ_v , and that of the maximum value at the largest ϵ_v . This suggests that the heat-pipe heat exchanger is not as good a device as it supposes to be as far as heat transfer is concerned. Care should therefore be taken in choosing the number and the alignment of heat pipes in engineering problems.

For all ten cases investigated the data seemed to correlate to a definite distribution shown in Fig. 3 which can be represented in the form of equation (4). However, c_1 and c_2 here are determined through the present numerical experiments.

For mass flow rate, ten out of twelve data from ref. [4] of numerical prediction for different ϵ_v s have been calculated and data were plotted as a function of ϵ_v . For clarification, the results of six from ten cases investigated are shown in Fig. 4. It can be seen that the variation of the mass flow rate has the same tendency as that of the heat transfer rate in Fig. 3. The present mass flow rate could then be represented in the form

$$\dot{m}_v = g_1(1 - e^{g_2 \epsilon_v})$$

where g_1 and g_2 were found to be very close to the values of \dot{m}_v calculated and c_1 , shown in Table 3, from equation (4) for the cases studied.

Two significant results are immediately apparent. One is

Table 1. Specification of heat pipe exchanger and its alignment

side cross-section ($W \times H$)	$2.0 \times 2.2 \text{ m}^2$
number of columns, N_c	$2N_1 + 1; N_1 = 1, 2, \dots, 6$
number of rows, N_r	$2N_2 + 1; N_2 = 1, 2, \dots, 6$
total number of heat pipes, N_t	$N_1 + 1 + N_2(2N_1 + 1); N_1 = 1, \dots, 6; N_2 = 1, \dots, 6$
heat pipe diameter, d	0.0337 m
heat pipe area fraction, ϵ_v	$N_t 0.785d^2 / WH$
heat pipe arrangement	staggered
condenser length of heat pipe, L_c	0.305 m
evaporator length of heat pipe, L_e	0.305 m
pipe pitch:	
longitudinal, S_H	$W/2^{N_1} \text{ m}$
transverse, S_V	$H/2^{N_2} \text{ m}$
frontal cross-section:	
for hot flow	$0.305 \times 2.2 \text{ m}^2$
for cold flow	$0.305 \times 2.2 \text{ m}^2$

Table 2. Calculation of heat transfer rate of Q_o and Q_s for different runs (data of test runs based on the data from ref. [4])

Test run no.	Hot air		Cold air		Heat transfer rate (W)	
	Flow rate (SCMM)	Inlet temp., $T_{h,i}$ (°C)	Flow rate (SCMM)	Inlet temp., $T_{c,i}$ (°C)	Q_s	Q_o
1	12.9	244.1	13.2	25.1	10512.0	7328.0
2	12.8	240.0	13.0	25.2	10310.4	7131.7
3	12.2	276.2	12.7	24.8	12067.2	8301.6
4	9.10	297.1	10.4	28.8	12818.4	8260.5
5	9.10	295.7	10.3	28.7	12816.0	8220.5
6	12.3	274.4	7.20	32.0	11635.2	7397.5
7	11.5	261.6	7.00	31.7	11035.2	7156.0
8	11.3	298.5	7.20	33.0	12744.0	8120.4
9	8.20	299.0	7.10	31.3	12849.6	7674.5
10	8.20	300.7	7.10	31.4	12926.1	7720.3

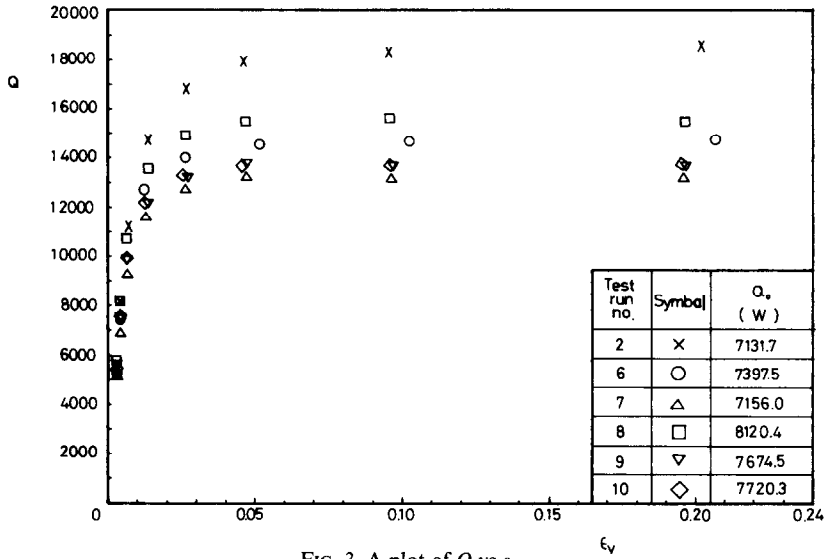


FIG. 3. A plot of Q vs ϵ_v .

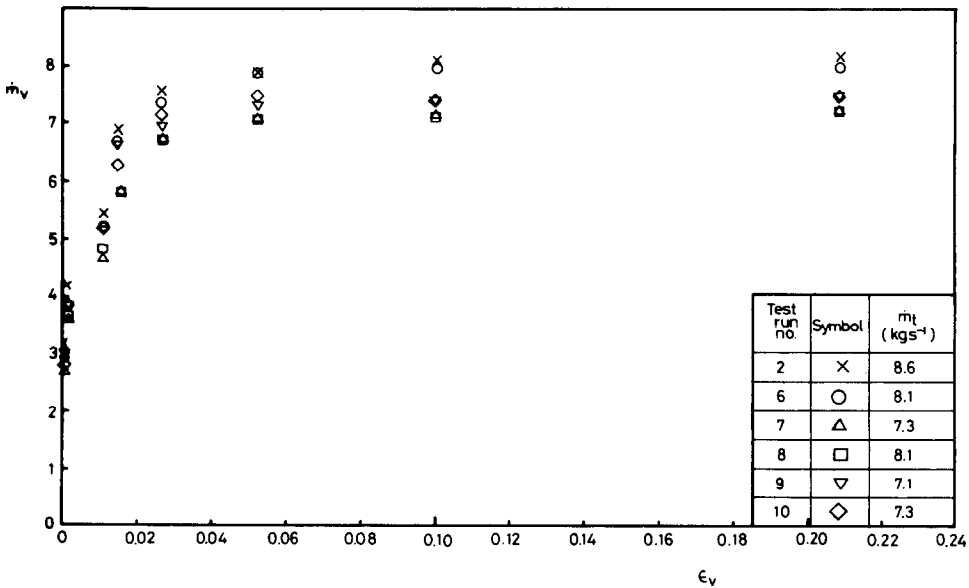


FIG. 4. Correlation of m_v and ϵ_v .

Table 3. Tabulated values of variables and correlating constants

Variables or constants	Test run no.										Average	Error
	1	2	3	4	5	6	7	8	9	10		
C_1	2.72	2.72	2.63	2.18	2.17	2.23	2.08	2.14	1.90	1.90	2.27	$\pm 20\%$
C_2	-200.6	-189.2	-179.8	-233.2	-233.8	-222.0	-257.0	-249.2	-272.2	-273.0	-231.0	$\pm 20\%$
g_1	8.9	8.6	9.9	8.3	8.2	7.8	6.9	8.3	6.8	6.9	8.1	$\pm 22\%$
g_2	-191.0	-190.9	-193.3	-218.5	-218.9	-256.3	-286.3	-292.7	-253.1	-252.6	-253.4	$\pm 17\%$
\dot{m}_i	8.6	8.4	9.8	9.1	8.5	8.1	7.3	8.1	7.1	7.3	8.2	$\pm 13\%$
\dot{h}_{fg}	2217.9	2196.3	1989.9	1876.4	1936.2	2074.5	2167.3	1985.7	1983.1	1792.4	2021.4	$\pm 11\%$

that the present correlation for both heat transfer and mass flow rates is consistent with each other as far as the correlating constants illustrating the thermal characteristics of the present heat-pipe heat exchangers are concerned. The other is that the heat transfer rate seems uniquely determined once \dot{m}_i and c_1 are found. It appears that the methodology under investigation does not generate any more limitations on the heat transfer rate of a heat-pipe heat exchanger.

The total mass flux as well as the average latent heat are also tabulated in Table 3 for ten cases with the maximum error about $\pm 20\%$. The error in the variable and the correlating constant was defined as the percentage deviation between the average value for total test runs and the value of each individual case. It is, therefore, concluded that the desired correlation for the heat transfer rate of a heat-pipe heat exchanger under the present configuration can be expressed in the form of

$$\frac{Q}{Q_0} = c_1(1 - e^{c_2 \dot{m}_i})$$

where $c_1 = 2.27 \pm 20\%$, $c_2 = -231.0 \pm 20\%$. It seems that c_1 and c_2 are independent of the specifications of the individual heat pipe. Further studies may include the experimental verification of the present results.

CONCLUSIONS

A simplified but relatively generalized method is developed and used to predict the thermal performance of the heat-pipe

heat exchanger for any staggered type alignment. The model has been tested based on the results from previous investigators. The resultant thermal performance is correlated in the form

$$\frac{Q}{Q_0} = 2.27(1 - e^{-231\dot{m}_i})$$

which may provide thermal design data for a heat-pipe heat exchanger configuration applicable to waste heat recovery systems.

Acknowledgements—The author would like to express his appreciation to Mr S. S. Liou for performing the numerical calculations for this study. Special thanks go to Mr C. T. Liah for typing the manuscript.

REFERENCES

1. S. W. Chi, *Heat Pipe Theory and Practice*, Chap. 1. McGraw-Hill, New York (1976).
2. J. O. Amode and K. T. Feldman, Preliminary analysis of heat pipe heat exchangers for heat recovery, ASME Paper No. 75-WA/HT-36 (1976).
3. Y. Lee and A. Bedrossian, The characteristics of heat exchangers using heat pipes or thermosyphons, *Int. J. Heat Mass Transfer* **21**, 221-229 (1978).
4. B. J. Huang and J. T. Tsuei, A method of analysis for heat pipe heat exchangers, *Int. J. Heat Mass Transfer* **28**, 553-562 (1985).

Radiative cooling of a solidifying droplet layer including absorption and scattering

ROBERT SIEGEL

NASA-Lewis Research Center, MS 5-9, Office of the Chief Scientist, 21000 Brookpark Road,
Cleveland, OH 44135, U.S.A.

(Received 1 December 1986 and in final form 17 February 1987)

INTRODUCTION

A POWER generating device for space applications requires a radiator for waste heat dissipation. As the power requirements increase (e.g. for a space station), a conventional radiator, such as a tube and fin design, could become so large and heavy that it would be impractical to launch and erect in space. A radiator has been proposed in the literature that may be much lighter and easier to deploy; it would utilize streams of hot liquid drops passing directly through space so that energy would be lost by transient radiative cooling

[1]. Recent research and analysis on this type of radiator are given in refs. [2-4]. To better utilize the energy transport ability of the drops, it may be useful to have the drops solidify, thereby taking advantage of their latent heat of fusion. This could also reduce evaporation losses from the drops. The liquid drop radiator would consist of thousands of individual directed streams that form a layer of drops (Fig. 1). If the initial temperature of this array of drops is near their freezing point, the subsequent radiative cooling will initiate solidification. During the phase change that follows, the two-phase layer will remain at uniform tempera-